

THE EFFECT OF THE EXCITATION VOLTAGE RISE TIME ON THE CHARACTERISTICS OF THE CORONA DISCHARGE

Ali Hussein Ali^{1*}, Qais Thanoun Al Jawari²

^{1*}Department of Physics, College of Education for Pure Sciences, University of Mosul, Mosul, Iraq

²Department of Physics, College of Electronics Engineering, Nineveh University

E-mail: ^{1*}alaa7usain@gmail.com, ²qais.najim@uoninvah.edu.iq

(Received September 10, 2022; Accepted November 21, 2022; Available online March 01, 2023)

DOI: [10.33899/edusj.2022.135797.1275](https://doi.org/10.33899/edusj.2022.135797.1275), © 2023, College of Education for Pure Science, University of Mosul.

This is an open access article under the CC BY 4.0 license (<http://creativecommons.org/licenses/by/4.0/>)

ABSTRACT:

In the current paper, the rise time of the exciting voltage on the characteristics of the DC corona discharge in a coaxial electrode system is presented. The current one-dimensional simulation study focused on the distribution of the plasma species (ions and electrons as well as the excited atoms) during two different times of the applied voltage climb was classified as a fast rise time (615 ns) and a slow rise time (2710 ns). The growth time of the corona excited voltage was controlled by the external feed RC circuit that connected with the central electrode. The simulation results have reveal that the corona inception which occurs at a fast rise time produces more dense plasma charged species, while the density of the excited atoms is not much affected by the applied voltage climb time. The density of excited atoms tends more to depend on the rise time of the exciting voltage at the steady state.

Keywords: Voltage rise time, Corona discharge, excited atoms

تأثير زمن ارتفاع الجهد المحفز على خصائص تفريغ الهالة

علي حسين علي^{1*}، قيس ذنون الجوّاري²

^{1*}قسم الفيزياء، كلية التربية للعلوم الصرفة، جامعة الموصل، الموصل، العراق

²قسم الفيزياء، كلية هندسة الالكترونيات، جامعة نينوى، الموصل، العراق

الخلاصة

في هذا البحث ، تم عرض تأثير زمن ارتفاع الجهد المطبق على خصائص تفريغ الاكليل للتيار المستمر في تكوين قطب كهربائي متحد المحور. ركزت دراسة المحاكاة الحالية ذات البعد الواحد على التوزيع المكاني للأيونات والإلكترونات وكذلك الأنواع المتحمسة خلال زمن الصعود السريع (615 نانوثانية) ووقت الارتفاع البطيء (2710 نانوثانية) لجهد التفريغ المطبق. تم التحكم في وقت ارتفاع الجهد المطبق بواسطة دائرة RC المتصلة بالقطب الكهربائي المركزي. تكشف نتائج المحاكاة أن بداية الهالة التي تحدث في وقت ارتفاع سريع تنتج أنواعًا مشحونة بالبلازما أكثر كثافة ، بينما لا تتأثر كثافة الذرات المثارة كثيرًا بزمن ارتفاع الجهد المطبق. تميل كثافة الذرات المثارة إلى الاعتماد على وقت ارتفاع الجهد المثير في الحالة المستقرة (أي عندما يصل الجهد المطبق إلى قيمة الذروة الثابتة). تصريفات الهالة من أهم أنواع البلازما المتأينة ويمكن تصنيفها ضمن فئة التفريغ الضعيف التأين. تستخدم العمليات الصناعية المختلفة تصريفات الهالة. تعتمد العديد من هذه التطبيقات على قدرة إنتاج تفريغات الهالة في الهواء عند الضغط القياسي (1 جو) ، وهو ضغط مرتفع نسبيًا لعمليات التفريغ الكهربائية بشكل عام. تتطلب العديد من تطبيقات تفريغ الهالة ذات

الضغط الجوي العملية التركيز على انتاج الانواع الفعالة للبلازما لتحقيق معالجة فعالة كبيرة. بعض هذه التطبيقات هي معالجة الأغذية والتطبيقات الطبية الحيوية.

الكلمات المفتاحية: الجهد، الزمن، الفولتية، الهالة الكهربائية

INTRODUCTION

Corona discharges are one of the most important types of ionized plasma and they can be categorized in the class of weakly ionized discharge. When a high positive or negative electric potential is provided at the sharp conductor, the neutral gas surrounding the sharp electrode (cathode) is ionized and subjected to electron drift as a result of the high electric field produced by the interaction of the high potential and short conductor curvature radius. Different industrial processes use corona discharges. Numerous of these applications are predicated on the ability to create corona discharges in air at standard pressure (1 bar), which is a relatively high pressure for electrical discharges in general. Many practical atmospherically pressure corona discharge applications require a high plasma chemical to achieve large effective processing. Some of these applications are food treatment and biomedical applications [1]. The application of the corona discharge proved to have a positive influence in this field of cold plasma applications [2]. Plasma chemical species can extinguish different microorganisms, destroying not just their membranes but also the DNA of bacteria and viruses [3]. Corona discharge can occur in both AC and DC high voltage systems. In comparison to corona discharges induced by AC high voltage sources, quick rise time high voltage pulses are known to provide greater plasma-chemical efficiency and a smaller average gas temperature rise [4-7]. The high density of plasma chemicals is desirable in many applications. The climb time of applied voltage plays a vital role in the corona discharge characteristics and especially the discharge current in the negative corona [8]. In the current study, we investigated the excitation of corona discharge in helium gas in a coaxial electrodes system for diverse rise times of the applied voltage and the impact of the excitation rise time on the spatial distribution of the excited atoms.

NUMERICAL MODEL

In the current model, a coaxial electrode system, similar to the system of reference [8], filled with pure Helium gas at atmospheric pressure was considered. The applied voltage is a DC with V_{peak} equal to -1 kV that energizes the central electrode of radius r_i . The length of the inner electrode was taken as dz 0.1 mm. The distance between the electrodes is 50 mm. RC circuit has been connected in series with the system to stop this avalanche from growing unabatedly. Based on the features of the external circuit, the voltage which feeds to the central electrode can be raised from the zero to the maximum value for various rise times. There are two types of rising times: quick and slow rise times. The well-known hydrodynamic model is used to create the governing equations for this model [9-11]. Comsol multiphysics was used to solve the governing equation. The set of continuity equations was taken into consideration in determining the generation and dissipation rates of the primary three main discharge species, namely positive ions, electrons, and excited atoms. The primary elements of the model equations that describe how electrons and other species entities migrate are diffusion and drifting velocity. Poisson's equation may be used to calculate how the accumulation of space charges will impact the electrical field. In the current model, we neglected the convection of electrons brought on by fluid motion. For the solution of the electrical potential and charged species, Poisson's equation and the continuity equations have been used respectively [10]:

$$\frac{d}{dt}(n_e) + \nabla \cdot [-n_e(\mu_e \cdot \vec{E}) - D_e \cdot \nabla n_e] = S_e \quad (1)$$

$$\frac{d}{dt}(n_p) + \nabla \cdot [-n_p(\mu_p \cdot \vec{E}) - D_p \cdot \nabla n_p] + E \cdot \Gamma_e = S_p \quad (2)$$

Where S_e is the electron source and the energy loss due to inelastic collisions and S_p will define later. E is the electric field. The electron diffusivity D_e , and energy diffusivity are computed from the electron mobility μ_e using the relations:

$$D_e = \mu_e T_e \quad (3)$$

$$D_p = \frac{5}{3} \mu_e T_e \quad (4)$$

T_e is the electron temperature. The plasma chemistry uses rate coefficients to derive the source coefficients in the aforementioned equations. The equation of the mass fraction is solved for non-electron species. The electrostatic field is calculated by the equation;

$$\nabla \cdot \epsilon \nabla V = -\rho \quad (5)$$

The combination of charge particles density ρ between the electrodes greatly affects the distribution of the Laplace field and can be calculated by equation 5. In general, the distance between the powered and grounded electrodes in the corona discharge system can be divided into two regions. The first region is the region of the ionization process, which is a small region around the powered electrode where the reactions of producing positive ions occur. The second region is the region of electron diffusion towards the ground electrode. The boundary conditions of positive ions are determined based on the continuity equation the density of positive ions is zero at the cathode and ground as for the boundary conditions of the electron. It consists of two conditions: the first is that the rate of change of the electron density at the ground electrode is zero and the second condition depends on the number of secondary electrons emitted from the cathode resulting from the collision of positive ions with the cathode and the secondary emission coefficient.

$$n_{sec} = \gamma n_{pc} \frac{\mu_p}{\mu_e} \quad (6)$$

Where n_{sec} represents the density of the on the electrode and n_{pc} is the density of positive ions on the electrode. The value of γ was taken equal to 0.001 [8]. In the current model, a pure *He* gas is used as a discharge gas under atmospheric conditions. Three main species were considered in the current model included positive ions, excited, and electrons. The list of the plasma species reactions was taken from Zhang et al., [12]. During this model, the working helium gas temperature is preserved constant at (293 °K).

RESULTS AND DISCUSSION

The coaxial discharge system was excited by a negative high voltage of 1 kV via the RC circuit which connected with the powered electrode. The rise time of the applied voltage was controlled by varying the value of R where the C is kept constant at 1 pF.

Fast rise time:

Using 100 kΩ for the series resistance produces a rise time of the applied voltage of 615 ns. To investigate the behavior of the charged species and the excited helium atoms before and after the corona inception, the densities of these species were analyzed at different stages of the applied voltage. In the following discussion, the characteristics of the corona discharge will be examined during the rise time of the applied voltage at five-time intervals which are the times that correspond to values (10% 25% 50% 75% 100%) of the applied voltage. Figure 1 shows the applied voltage during the fast and slow rise time.

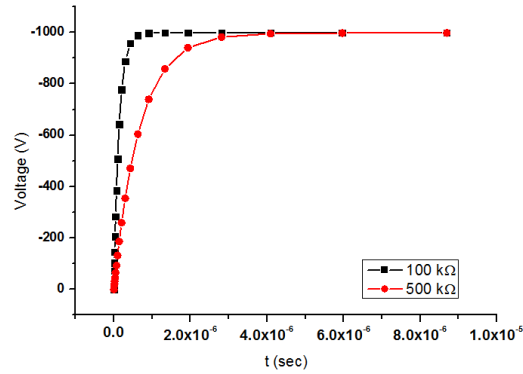


Fig. 1. Applied voltage during the fast and slow rise time

1. $t=1.46 \times 10^{-8}$ s (when $V_{app} = 10\%$ of V_p)

At this time the applied voltage which represents 10% of the maximum voltage, and the density of electrons, excited atoms, and positive ions are shown in figure 1. It can be observed a constant distribution of all the plasma species along the distance between the electrodes and the value of these particles is in the range of the initial value. The uniform distribution indicates that the applied voltage is much less than the corona inception voltage. A remarkable notice in figure 2 is that there is a decrease in the electron density near the powered electrode due to the negative applied voltage.

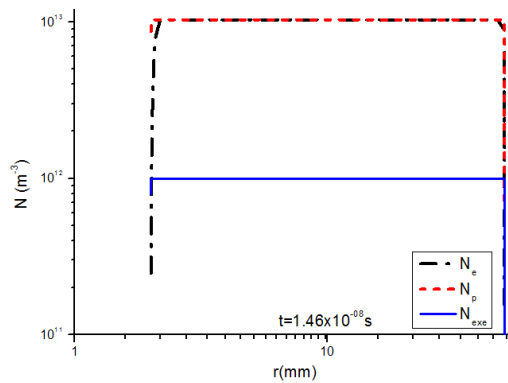


Fig. 2. Electrons, positive ions and excited atoms spatial distribution along the distance between the electrodes at $t=1.46 \times 10^{-8}$ s ($V=10\%$ V_p)

2. $t=1.46 \times 10^{-8}$ s (when $V_{app} = 25\%$ of V_p)

As time goes on the applied voltage increase and it reaches 25% from the maximum value at $t=1.46 \times 10^{-8}$ s. Figure 3 depicted, that at this time, the density of electrons decreases in the vicinity of the discharge electrode due to the action of applied negative potential. The electrons start to move towards the ground electrode but since that applied voltage is still under the inception voltage, therefore the electrons cannot gain enough energy for excitation and ionization processes. So, the density of the ions and excited atoms is almost constant along the discharge channel where its values are in the range of initial values.

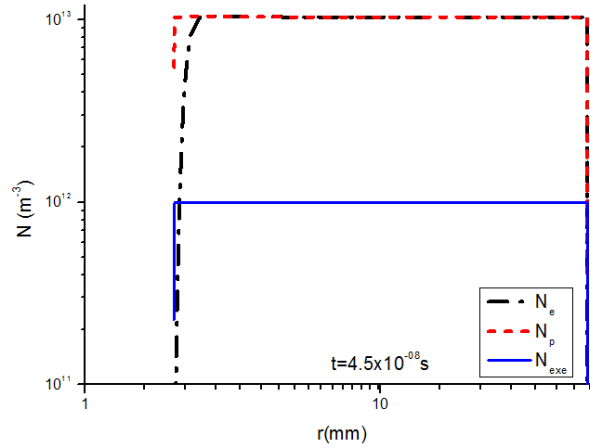


Fig. 3. Electrons, positive ions and excited atoms spatial distribution along the distance between the electrodes at $t=4.5 \times 10^{-8}$ s ($V=25\% V_p$)

3. $t=9.54 \times 10^{-8}$ s (when $V_{app} = 50\%$ of V_p)

At this time, the applied voltage reaches 50% of the peak value. The spatial distribution of plasma species is shown in figure 4. It can be seen that the clouds of electrons and positive ions are created near the powered electrode ($R \approx 2$ mm) due to the ionization processes. Under the effect of the applied electric field, the electrons move away from the central electrode gaining enough ionization energy. This is revealed clearly by an increase in the positive ion density. The generated positive ions drift toward the discharge electrode under the influence of the applied voltage. The increase in the density of the electrons and positive ions indicates that the applied voltage reached the corona inception voltage. Figure 3 illustrates that the density of the excited atoms is still in the range of the initial value with a uniform distribution between the electrodes. However, this can be ascribed to the non-uniform electric field that gives sufficient energy to the initial electrons to produce ionization processes rather than excitation.

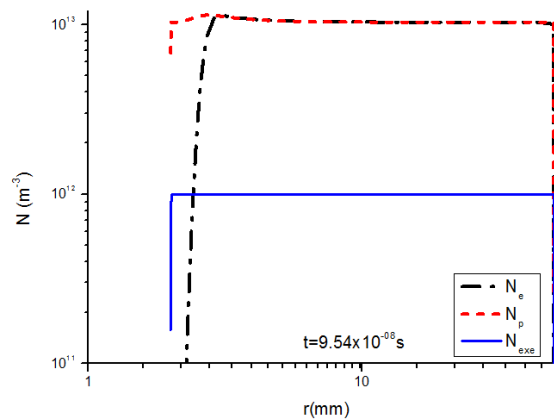


Fig. 4. Electrons, positive ions and excited atoms spatial distribution along the distance between the electrodes at $t=9.54 \times 10^{-8}$ s ($V=50\% V_p$)

4. $t=20.2 \times 10^{-8}$ s (when $V_{app} = 75\%$ of V_p)

Figure 5 depicts the spatial distribution of the electrons, ions, and excited atoms when the applied voltage reaches 75% of the peak value. It can be noticed that the continuation of the movement of electrons away from the negative voltage electrode and drifting towards the ground electrode. A noticeable separation between the electrons swarms from the positive ions with increasing in the

density of both types of charged species. Although at this time, the applied voltage reached the corona inception voltage while the density of the excited atom is still unaffected by the local charge creation.

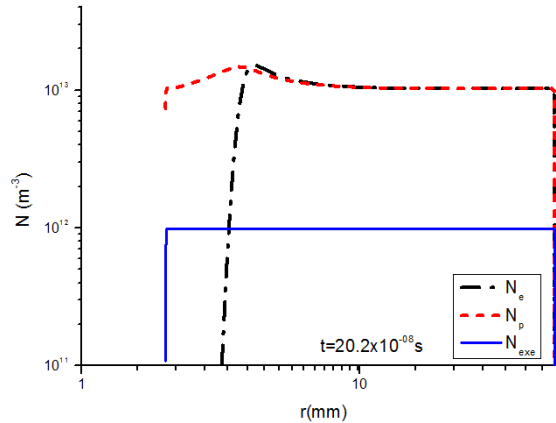


Fig. 5. Electrons, positive ions and excited atoms spatial distribution along the distance between the electrodes at $t=20.2 \times 10^{-8}$ s ($V=75\% V_p$)

5. $t=8.69 \times 10^{-6}$ s (when $V_{app} = V_p$)

At $t=8.69 \times 10^{-6}$ s, the applied voltage reaches the maximum applied voltage. As shown in figure 5, the separation between the positive ions and electrons clouds becomes very obvious. In addition to that, a noticeable increase in the density of the positive ions can be observed along with the discharge channel. The peak of the positive ions cloud can be seen at ($R=2$ mm) from the corona electrode. Figure 6 reveals the uneven distribution of the electrons along the distance between the electrodes. It can be also seen that there are two peaks of the electrons with unequal amplitude. The maximum peak is located after the mid-gap between the electrodes ($R \sim 15$ mm) which is resulted from electron diffusion far away from the ionization region while the second peak is found located ($R \sim 15$ mm) from the powered electrode. The second peak could be resulted from secondary electrons emission from the cathode due to the positive ions bombardment. Although the applied voltage reached the maximum value, the density of excited atoms is still constant and in the range of the initial value. This indicates that the applied voltage variation with time gives high energy to the electrons to make ionization processes rather than excitation.

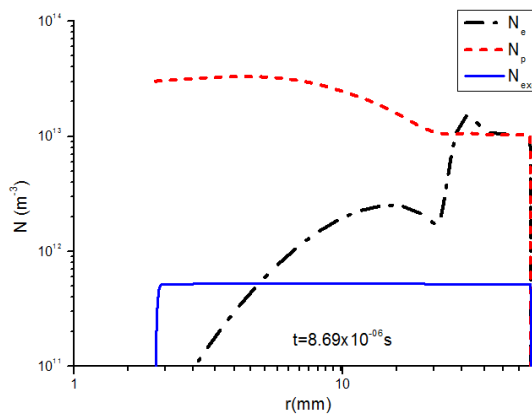


Fig. 6. Electrons, positive ions and excited atoms spatial distribution along the distance between the electrodes at $t=8.69 \times 10^{-6}$ s ($V=100\% V_p$)

After the time of the maximum value of the applied voltage (i.e., $t > 8.69 \times 10^{-6}$ s), the discharge reached the steady state with ($dV/dt = 0$). During this phase, the spatial distribution of the excited atoms was examined at different times. Figure 7 shows the distribution of helium excited atoms at $t=3.9 \times 10^{-7}$

⁵, 5.68×10^{-5} , 17.5×10^{-5} , and 15.1×10^{-4} s from the beginning of the applied voltage. It can be noticed the uneven distribution of the excited atoms along the distance between the electrodes during these times. The spatial behavior of the excited atoms reveals a peak close to the powered electrode located at ($R \sim 2.5$ to 3 mm). The density of these excited atoms decreases exponentially along the discharge channel. This distribution takes the shape of the electric field around the central electrode in the coaxial system. When the positive ions bombard the powered electrode, the released electrons start to accelerate in the non-uniform field. After a short distance and due to the high electric field it acquired enough energy to excite the helium atoms and thus a peak of the excited atoms is obtained.

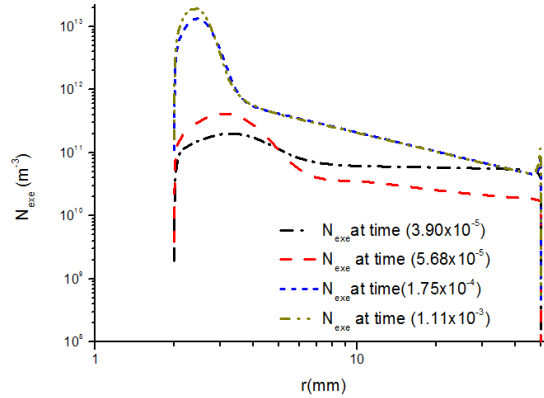


Fig. 7. Electrons, positive ions and excited atoms spatial distribution along the distance between the electrodes at different times during the applied voltage steady state (for fast time of applied voltage).

Slow rise time:

To get a complete vision of how the rise time of the applied voltage impacts the density of the excited atoms in a helium corona discharge, the series resistor with the inner corona electrode was changed to 500 ohm. This resistance produces a rise time of 2710 ns, which is slow compared to the last case.

1. $t = 2.12 \times 10^{-8}$ s (when $V_{app} = 10\%$ of V_p)

When the applied voltage rises to 10% of the maximum voltage, the spatial distribution of the plasma charged species and excited atoms show similar behavior to what was observed in the case of fast rise time as shown in figure 8. This happen because there is not much difference in the rise time of the applied voltage during this short time.

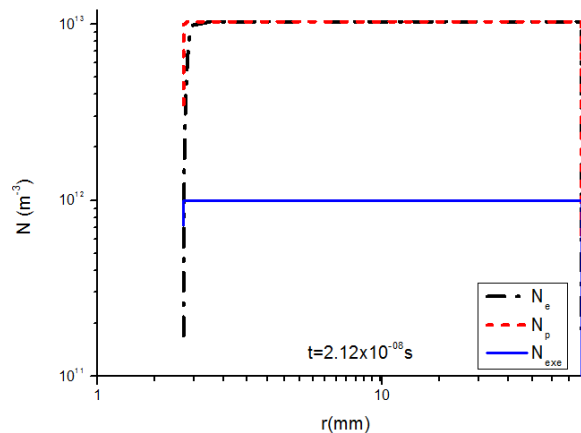


Fig. 8. Electrons, positive ions and excited atoms spatial distribution along the distance between the electrodes at $t = 2.12 \times 10^{-8}$ s ($V = 10\% V_p$)

For better differentiation, it is good to examine the spatial distribution of the plasma species at the time of V_{app} is equal to 50% of V_p .

2. $t=91.0 \times 10^{-8}$ s (when $V_{app} = 50\%$ of V_p)

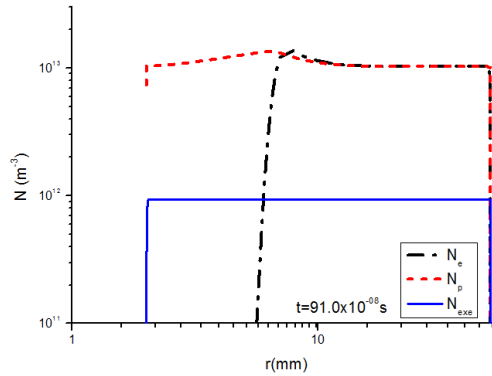


Fig. 9. Electrons, positive ions and excited atoms spatial distribution along the distance between the electrodes at $t=91.0 \times 10^{-8}$ s ($V=50\%$ V_p)

Figure 9 depicts the electrons, ions, and excited atom's distribution along with the discharge channel during the time at which the applied voltage reached 50% of its maximum value. It can be seen that until this time the applied voltage is not enough to create a noticeable difference in the species distribution. This could be attributed to the low value of (dV/dt) which cannot give enough energy to electrons to produce excitation or ionization.

3. $t=9.10 \times 10^{-7}$ s (when $V_{app} = 75\%$ of V_p)

The applied voltage reached 75% of its highest value during this time, $t=9.10 \times 10^{-7}$ s. As shown in figure 10, the electron density is affect clearly with the applied voltage where the density of the electrons shows a peak value at $d \sim 10$ mm from the cathode with a peak value of 10^{13} cm^{-3} . This position of the peak value of the cloud of electrons is located at distance far from the case of fast rise time. This happened because the electrons can travel a great distance away from the cathode during the slow rise climb of the applied voltage.

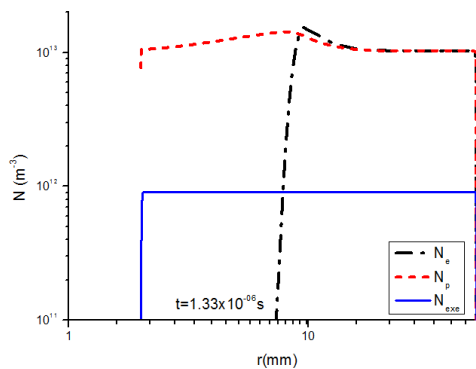


Fig. 10. Electrons, positive ions and excited atoms spatial space along the distance between the electrodes at $t=1.33 \times 10^{-6}$ s ($V=75\%$ V_p)

4. $t=8.6 \times 10^{-6}$ s (when $V_{app} = V_p$)

When the applied voltage reaches the peak value after a long time compared to the previous case, the characteristics of the corona discharge along the distance between the electrodes show different behaviors. As illustrated in figure 11, there is no clear peak for the positive ions cloud like what was

obtained in figure 5 for the case of the fast climb time of the corona excited voltage. In addition to that the density of the positive ions is less than the density in the previous case. The electrons distribution shows also a difference from the case of the fast rise time. The peak of the electrons cloud is located at distance near the ground electrode with less density compared to the case of the fast rise time of the applied voltage.

For all the aforementioned times of the corona excited voltage, the density of the excited atoms shows no obvious difference from the last case. This indicates that the electron excitation reactions do not play a significant role during the voltage development phase.

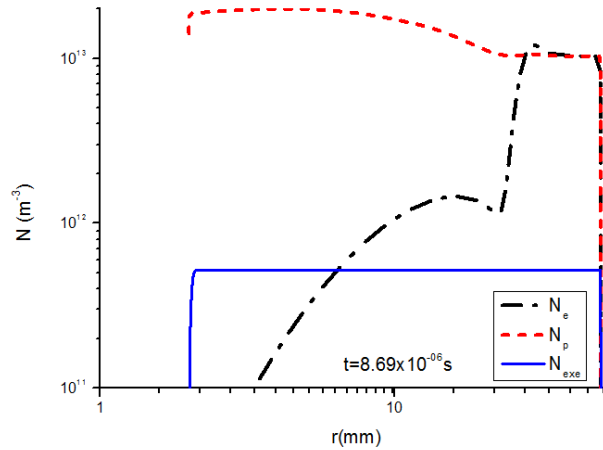


Fig. 11. Electrons, positive ions and excited atoms spatial distribution along the space between the electrodes at $t=8.69 \times 10^{-6}$ s ($V=100\% V_p$)

By comparison with the previous case, the spatial distribution of excited helium atoms was examined during the voltage steady state (i.e., $dV/dt = 0$) at different times.

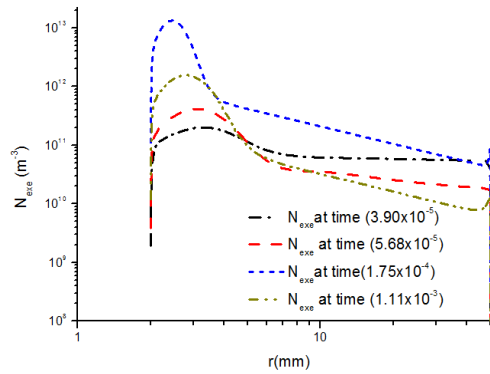


Fig. 12. Electrons, positive ions and excited atoms spatial distribution along the space between the electrodes during the steady state of the applied voltage (for slow time of applied voltage)

Figure 12 shows the distribution of helium excited atoms at $t=3.9 \times 10^{-5}$, 5.68×10^{-5} , 17.5×10^{-5} , and 15.1×10^{-4} s from the beginning of the applied voltage. It can be noticed that the distribution of the excited atoms along the distance between the electrodes is similar to the distribution of the excited atoms in the case of the fast climb time of the corona excited voltage. The spatial behavior of the excited atoms reveals a peak close to the powered electrode located at ($R \sim 2.5$ to 3 mm). The main difference is the excited atoms in the current case are lower than in the previous one. This indicates that the number of positive ions that collide with the cathode is less than the case of fast rise time of the applied voltage. The relatively low production of the excited atoms during the slow rise time of the applied voltage compare with the case of the fast rise time is similar to what was obtained by Lei I weke et al., [13] in a high pressure dielectric barrier discharge.

CONCLUSIONS:

The present work has reports the numerical simulation of the corona discharge in coaxial electrode configuration at atmospheric pressure. The study focused on the role of the growth time of the applied voltage on the plasma characteristics. In a nutshell, this paper showed that using the slow rise of the excited voltage in the coaxial corona discharge system has produced a relatively low density of electrons and positive ions compared with the fast growth time of the applied voltage. For both cases of the rise time (fast and slow) of the applied voltage, and during the time of voltage rise up, the density of excited atoms is still unaffected. When the applied voltage reached the steady state, an increase in the density of the excited atoms is obtained. Under the case of the voltage steady state, the excited atoms which are produced by fast rise time are higher than the excited atoms are produced by slow rise time.

ACKNOWLEDGEMENT

One of the authors (Ali H. A) thanks all the staff and lecturers in the Department of Physics in Education for Pure Sciences at the University of Mosul, who helped me on my study journey.

REFERENCES:

1. R. Thirumdas, "Exploitation of cold plasma technology for enhancement for seed germination," *Agricul. Res. Technol. Open access j.*, vol. 13, no. 2, pp. 25-29, 2013
2. B. Adhikari, and G. Park, "The effects of plasma on plant growth, development, and sustainability," *Appl. Sci.* no. 10, pp. 6045- 6064, 2020.
3. V.L. Bychkov, A.R. Bikmukhametova, V.A. Chernikov, and et.al., "Corona Discharge Influence on Soil," *IEEE Trans. Plasma Sci.*, vol. 48, no. 2, pp. 350-354, 2020. DOI 10.1109/TPS.2019.2960230
4. K. Okazaki and T. Nozaki, *Pure Appl. Chem.* **74**, 447 2002.
5. R. J. Leiweke and B. N. Ganguly, Temperature measurement in a high pressure dielectric barrier discharge using pressure induced line broadening and frequency shift, *Appl. Phys. Lett.* **88**, 131501 2006.
6. J. M. Williamson, D. D. Trump, P. Bletzinger, and B. N. Ganguly, *J. Phys. D*, Comparison of high-voltage ac and pulsed operation of a surface dielectric barrier discharge. **39**, 4440 2006.
7. R. P. Mildren, R. J. Carman, and I. S. Falconer, Visible and VUV emission from a xenon dielectric barrier discharge using pulsed and sinusoidal voltage excitation waveforms. *IEEE Trans. Plasma Sci.* **30**, 192 2002.
8. D. N. Saleh, Q. Th. Algwari, and F. Kh. Amouri, "Modeling the dependence of the negative corona current density on applied voltage rise time" *Phys. Plasmas* **27**, 073501, 2020
9. G. Georghiou, A. Papadakis, R. Morrow, and A. Metaxas, "Numerical modeling of atmospheric pressure gas discharges leading to plasma production, *J. Phys. D* **38**, R303, 2005.
10. J. Chen and J. Davidson, "Model of the negative DC corona plasma: Comparison to the positive DC corona plasma," *Plasma Chem. Plasma Process.* **23**, 83, 2003.
11. Y. Yi, W. Tang, Z. Chen, and L. Wang, "A full hydrodynamic steady-state model of positive DC corona in coaxial cylindrical electrode," *Phys. Plasmas* **25**, 063526, 2018
12. Y. T. Zhang, D. Z. Wang and M. G. Kong, "Two-dimensional simulation of a low-current dielectric barrier discharge in atmospheric helium" *Journal of Applied Physics* **98**, 113308, 2005
13. R. J. Leiweke and Biswa N. Ganguly, "Effects of pulsed-excitation applied voltage rise time on argon metastable production efficiency in a high pressure dielectric barrier discharge" *Appl. Phys. Lett.* **90**, 241501, 2007